Frontiers in Bioscience Landmark

Front. Biosci. (Landmark Ed) **2026**; 31(2): 47824
https://doi.org/10.31083/FBL47824

Original Research

ITPR2 Promotes Acute Myeloid Leukemia Progression Through Calcium-Mediated Mitochondrial Dysfunction

Xiaoke Huang[1,2,†], Na Lu[1,†], Shanhu Zhu[1], Xiaolin Liang[1], Yiqian Huang[1], Jiamin Luo[1], Zhenfang Liu[1,*]

[1]Department of Hematology, The First Affiliated Hospital of Guangxi Medical University, 530021 Nanning, Guangxi, China
[2]Key Laboratory of Hemotology, Guangxi Medical University, Education Department of Guangxi Zhuang Autonomous Region, 530021 Nanning, Guangxi, China
*Correspondence: liuzhenfang@gxmu.edu.cn (Zhenfang Liu)
[†]These authors contributed equally.
Academic Editor: Christian Borgo
Submitted: 30 October 2025 Revised: 3 January 2026 Accepted: 9 January 2026 Published: 13 February 2026

Abstract

Background: Acute myeloid leukemia (AML) is a hematological malignancy of the myeloid lineage with poor clinical outcomes due to limited targeted therapies. This study elucidates the role of inositol 1,4,5-trisphosphate receptor type 2 (*ITPR2*) in regulating cell apoptosis by modulating mitochondrial calcium (Ca^{2+}) levels and underscores the clinical significance of *ITPR2*. **Methods**: *ITPR2* expression in patients with AML compared with that of healthy controls using the quantitative real-time PCR (RT-qPCR) method. The role of *ITPR2* in AML and its association with immune infiltration levels were investigated through bioinformatics analyses. *ITPR2* knockdown in Tohoku Hospital Pediatrics-1 (THP-1) cells were achieved using small interfering RNA (siRNA) and 2-aminoethyl diphenylborinate (2-APB), followed by comprehensive molecular characterization employing RT-qPCR, western blotting (WB), cell counting kit-8 (CCK-8) assays, and flow cytometry. **Results**: *ITPR2* was validated as being highly expressed in patients with AML, and this expression correlated with risk stratification and poor prognosis. Functional enrichment analysis revealed that *ITPR2* is involved in Ca^{2+} signaling pathways and mitochondrial-related biological processes, and its expression level was negatively correlated with immune infiltration levels. Knockdown of *ITPR2* or inhibition of its activity with 2-APB reduced Ca^{2+} ion concentrations in both the cytoplasm and mitochondria, leading to mitochondrial dysfunction (characterized by elevated intracellular reactive oxygen species (ROS) levels, reduced mitochondrial membrane potential (MMP) levels, and reduced mitochondrial DNA copy number) and eventually AML cell apoptosis. **Conclusion**: *ITPR2* facilitates AML progression via the Ca^{2+}-mitochondrial axis and may serve as a prognostic factor and potential therapeutic target.

Keywords: acute myeloid leukemia; mitochondrial; calcium; prognosis

1. Introduction

The acute myeloid leukemia (AML) is a highly heterogeneous clonal malignancy of the haematopoietic system and the most prevalent form of acute leukaemia in adults [1]. Abnormal gene expression and mutations are central mechanisms that regulate the initiation and progression of AML. Although the clinical application of targeted therapeutic agents, such as FMS-like tyrosine kinase 3 (*FLT3*) inhibitors, isocitrate dehydrogenase 1/2 (*IDH1/2*), B-cell lymphoma-2 (*Bcl-2*) inhibitors, has broadened treatment options for AML [2], the overall survival (OS) of patients has not significantly prolonged. Therefore, there is an increasing clinical need to systematically clarify the core molecular mechanisms involving AML pathogenesis and to explore potential therapeutic targets with clinical translational value. This endeavor is of great scientific significance to explore new and effective treatment methods aimed at improving patient prognosis.

Inositol 1,4,5-trisphosphate receptors (*ITPRs*), crucial intracellular calcium (Ca^{2+}) ion channel proteins, are widely distributed in mammalian tissue cells, mediating Ca^{2+} ion release and signal transduction. The Ca^{2+} ion signaling pathway regulates fundamental physiological processes like cell proliferation, apoptosis, and differentiation [3,4]. Due to their central regulatory role, *ITPRs* are vital targets for understanding disease pathogenesis. Some investigators found that aberrant expression of *ITPRs* in solid tumors like breast cancer [5], cholangiocarcinoma [6], and renal cell carcinoma [7] correlates with advanced tumor stage and poor prognosis, suggesting their potential as diagnostic markers and therapeutic targets. Research on *ITPRs* in hematological diseases is limited. Our single-cell sequencing data revealed upregulation of inositol 1,4,5-trisphosphate receptor type 2 (*ITPR2*) in AML [8], consistent with prior reports [9], indicating a key oncogenic role of *ITPR2* in AML. Nevertheless, the biological functions and mechanisms of *ITPR2* in AML remain largely unknown.

This study reveals that *ITPR2* is significantly upregulated in AML, with its elevated expression associated with poor prognosis in AML patients. Mechanistically,

ITPR2 knockdown disrupts mitochondrial Ca^{2+} homeostasis, caused oxidative stress and mitochondrial dysfunction, which in turn promotes apoptosis in AML cells. These results clarify the fundamental role of *ITPR2* in AML, and provide essential experimental evidence for understanding the molecular mechanisms that underlie AML pathogenesis and for developing treatment methods targeting *ITPR2*.

2. Materials and Methods

2.1 Acquisition and Survival Correlation Analysis of ITPR2 mRNA Expression in AML Cohorts

This study downloaded the uniformly standardized pan-cancer dataset from the University of California, Santa Cruz Genomic (UCSC) database and extracted *ITPR2* expression data for each sample. Acute myeloid leukemia-M3 (AML-M3) samples were excluded, and all expression data were transformed to log2(x + 1) form. Differences in *ITPR2* expression between samples were analyzed using R software (version 4.2.1, R Foundation for Statistical Computing, Vienna, Austria) [10]. The association between *ITPR2* level and OS was investigated using data from the Gene Expression Omnibus (GEO) database (accession No: GSE12417; n = 242), with the median *ITPR2* level used as the threshold for grouping.

2.2 BM Samples

Bone marrow (BM) samples were obtained from 82 newly diagnosed AML patients and 30 normal donors at the First Affiliated Hospital of Guangxi Medical University, China, from 2013 to 2021. The diagnosis of AML was confirmed according to the World Health Organization (WHO) classification system. Ethical approval for this research was granted by the Ethical Review Commission of the First Affiliated Hospital of Guangxi Medical University, Nanning, China (Approval code: 2025-E0668).

2.3 Quantitative Real-Time PCR (RT-qPCR)

Bone marrow mononuclear cells (BM-MNCs) were isolated by centrifugation, from which total RNA was extracted. RNA purity was assessed via spectrophotometer, with a 260/280 nm ratio greater than 1.8 indicating adequate purity. The total RNA was then converted into complementary DNA by reverse transcription. Human β-actin serves as a reference gene to normalize. The relative levels of expression were calculated using the $2^{-\Delta\Delta Ct}$ method. The primer sequences were as follows: β-actin forward 5′-GTGGCCGAGGACTTTGATTG-3′ and reverse 5′-CCTGTAACAACGCATCTCATATT-3′, *ITPR2* forward 5′-TGCGCCAATCAGCTACTTCT-3′ and reverse 5′-TCAGGATTAAGCTCTGCAGCTA-3′.

2.4 Functional Enrichment and Immune Infiltration Analysis

ITPR2 expression data were extracted from The Cancer Genome Atlas–Acute Myeloid Leukemia (TCGA-LAML) (non-M3) database. The samples were divided into high and low expression groups based on the median *ITPR2* level. Differential expression analysis between the two groups was performed using the *limma* package, with differentially expressed genes (DEGs) judgement criteria of $|\log2FC| > 1$ and $p.adj < 0.05$. The enrichment analyses were subsequently performed on the R clusterProfiler package [11]. DEGs with $p.adj < 0.05$ were selected for differential expression analysis. The c2.all.v2022.1.Hs.symbols.gmt gene set (a standardized, curated gene set file from the molecular signatures (MSigDB), specifically designed for functional enrichment analysis in human [Homo sapiens] molecular biology and biomedical research) were obtained from the MSigDB database for Gene Set Enrichment Analysis (GSEA) [12]. The enriched pathway results met the thresholds of $p.adj < 0.05$ and a $q < 0.25$. The Estimation of Stromal and Immune cells in Malignant Tumor tissues using Expression data (ESTIMATE) algorithm was applied to calculate the immune infiltration score of the AML samples. The single sample gene set enrichment analysis (ssGSEA) algorithm was applied to determine the association between *ITPR2* level and the immune infiltration levels [13]. Finally, Pearson correlation analysis was conduct to clear the association between *ITPR2* level and 47 immune checkpoint-related genes [14]. The analysis results were visualized with R ggplot2 package [15].

2.5 Cell Culture

Tohoku Hospital Pediatrics-1 (THP-1) cells were acquired from the Shanghai Cell Bank (https://www.cellbank.org.cn). THP-1 cells were cultured in RPMI-1640 (Gibco, NY, USA) with 10% fetal bovine serum (FBS) (Biological Industries, Cromwell, CT, USA) and 1% penicillin-streptomycin at 37 °C. All cell lines were validated by STR profiling and tested negative for mycoplasma.

2.6 Small Interfering RNA (siRNA)

siRNA was used to silence the *ITPR2* gene. The plasmid construct was synthesized and generated by Guangzhou Ribobio Co., Ltd. (a commercial biotechnology company specializing in nucleic acid synthesis and vector construction). The interfering sequences targeting the *ITPR2* gene were as follows: siRNA-*ITPR2*-1: 5′-CAACGAAATTAGCGAGAGA-3′, siRNA-*ITPR2*-2: 5′-CCCTTAGCCTACCACATCA-3′, siRNA-*ITPR2*-3: 5′-GTGGCGCTTTCATGTCGAA-3′. THP-1 cells were seeded in 6-well plates and cultured until 50% confluency. Subsequently, transfection of 20 nM negative control siRNA (si-NC) with a scrambled sequence that does not target any human genes or *ITPR2*-specific siRNA into THP-1 cells was performed using the CALNP™ RNAi *in vitro* (Beijing D-Nano Therapeutics, Beijing, China) reagent at 37 °C for 24 h. Subsequently, at other indicated time points, the cells were harvested and stored.

2.7 Western Blot (WB)

Western Blot (WB) cellular proteins were lysed using radio-immunoprecipitation assay (RIPA) buffer and centrifuged for 5 minutes at 4 °C. Equal amounts of protein (40 µg) were loaded into each lane and separated by 10% SDS-polyacrylamide gel electrophoresis (SDS/PAGE). The proteins were then electrotransferred to a polyvinylidene fluoride (PVDF) membrane. The membranes were blocked via 8% nonfat milk for 1 h and overnight incubated with primary antibodies at 4 °C. The specific primary antibodies used in this study were: anti-ITPR2 (Affinity, CAT#DF13336, dilution ratio 1:1000), anti-Cyclin D1 (Proteintech, CAT#26939-1-AP, dilution ratio 1:2000), anti-Cyclin E1 (Proteintech, CAT#11554-1-AP, dilution ratio 1:2000), anti-CDK6 (Proteintech, CAT#14052-1-AP, dilution ratio 1:1000), anti-Bcl-2 (Proteintech, CAT#12789-1-AP, dilution ratio 1:4000), anti-Bax (Proteintech, CAT#50599-2-Ig, dilution ratio 1:5000), and anti-actin (Abcam, CAT#ab8226, dilution ratio 1:2000). After washing via phosphate-buffered saline (PBS), the membranes were incubated for 1 h with corresponding secondary antibodies (Anti-Rabbit IgG (Zenbio, CAT#511203, dilution ratio 1:5000) Anti-Mouse IgG (Zenbio, CAT#511103, dilution ratio 1:4000)) in a blocking solution. Chemiluminescence was detected using a kit from chemiluminescence detection kit (Bio-Rad) [16] with β-actin serves as a loading control. ImageJ software (v1.8, National Institutes of Health, Bethesda, MD, USA) was applied to determine the band intensity.

2.8 Cell Counting Kit-8 (CCK-8)

CCK-8 (NCM Biotech, Suzhou, Jiangsu, China) was utilized to evaluate cell viability. Ten microliters of CCK-8 were given each well and cultured for 2 h at 37 °C. The cells absorbance were detected with a spectrophotometer (Molecular Devices, San Jose, CA, USA) at 0, 24, 48, 72 h post-seeding.

2.9 Cell Cycle Phase Analysis

Cell Cycle Analysis Kit (Beyotime, Shanghai, China) was applied to conduct the cell cycle assessment. Cells were subjected to two rounds of washing with PBS. After that fixed them in ethanol at 4 °C for 12 hours. Subsequently, centrifuged at 800 rpm for 5 minutes, then stained with propidium iodide (PI) and RNase A, and incubated at 37 °C for 30 minutes without light. The stained cells were detected via the CytoFLEX flow cytometer (Beckman Coulter, Brea, CA, USA). G0/G1, S, and G2/M phase distribution were measured using FlowJo software (v10.8.1, FlowJo LLC, Ashland, OR, USA).

2.10 Apoptosis Assays

The Annexin V-Fluorescein Isothiocyanate (FITC) Apoptosis Detection Kit (Beyotime) was utilized to measure cellular apoptosis following the relevant interpretion. Cells from various groups were plated in 6-well plates, then collected and washed with PBS. Next, 195 µL of Annexin V-FITC binding solution was used to resuspend them. For each tube, 5 µL of Annexin V-FITC and 10 µL of PI were added, then cultured for 20–25 minutes without light. Apoptosis rates of cells from each group were evaluated by flow cytometry. Additionally, late apoptosis was evaluated via labeling DNA fragments of apoptotic cells with a Terminal Deoxynucleotidyl Transferase dUTP Nick-End Labeling (TUNEL) Assay Kit (Elabscience, Wuhan, China). Following fixation, permeabilization, equilibration, labeling, and washing per the instructions, detected with flow cytometer. TUNEL-positive cells were quantified with FlowJo software (v10.8.1).

2.11 Ca^{2+} Imaging

Fluorescent indicators Fluo-4 AM (Beyotime) and Rhod-2 AM (Yesen, Shanghai, China) were employed to determine the levels of cytoplasmic Ca^{2+} and mitochondrial Ca^{2+}, respectively. THP-1 cells were prepared as single-cell suspensions and loaded with 5 µM Fluo-4 AM and 5 µM Rhod-2 AM by incubation at 37 °C for 30 minutes. Then, the cells were washed with PBS to eliminate any extracellular Fluo-4 AM and Rhod-2 AM. The cytoplasmic and mitochondrial Ca^{2+} concentrations were then simultaneously measured by CytoFLEX flow cytometry (Beckman Coulter).

2.12 The Mitochondrial Membrane Potential (MMP) Assay

The MMP was assessed via flow cytometry with JC-1 staining, following the manufacturer's instructions (C2006, Beyotime) [17]. Cells were collected and resuspended in 0.5 mL of cell culture medium and then incubated with 0.5 mL of a JC-1 staining solution in the dark at 37 °C for 20 minutes. Then, the cells were harvested, washed three times with JC-1 staining buffer, and resuspended in JC-1 staining buffer. The red/green fluorescence of JC-1-labelled cells was detected using a CytoFLEX flow cytometry (Beckman Coulter). The difference in MMP were determined by the color transformation of the fluorescence.

2.13 Measurement of Reactive Oxygen Species (ROS)

Intracellular ROS levels were detected with a DCFH-DA probe (Beyotime). The cells were treated with serum-free media containing 10 µM DCFH-DA probe and incubated at 37 °C in the dark for 30 minutes, with gentle agitation every 5 minutes. After incubation, the cell pellets were collected, washed with PBS, and resuspended in PBS for CytoFLEX flow cytometry (Beckman Coulter) detection. The resulting green fluorescence was measured and the mean fluorescence intensity (MFI) serves as an indicator of the relative intracellular ROS levels.

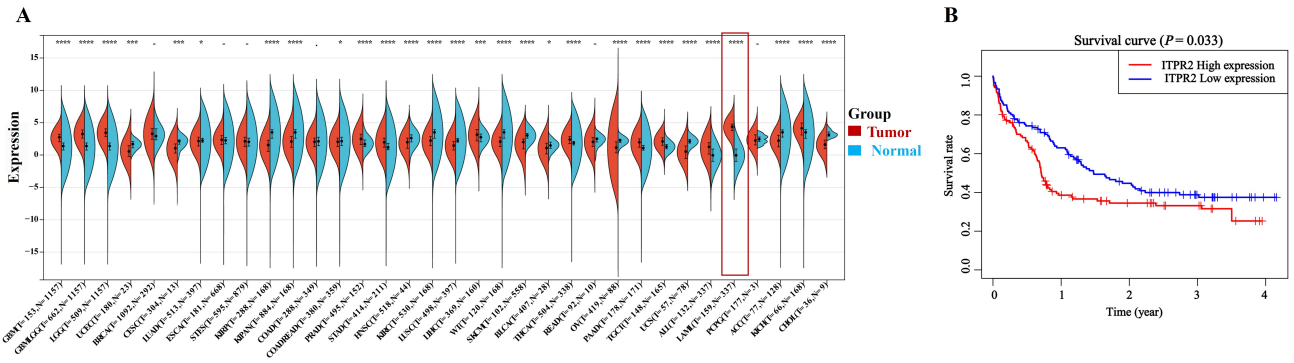

Fig. 1. *ITPR2* expression was increased in public databases vs. normal group and associated with prognosis. (A) Expression of *ITPR2* in pan-cancer. (B) OS of GSE12417 patients (n = 242) stratified by high vs. low *ITPR2* expression. * $p < 0.05$, *** $p < 0.001$, **** $p < 0.0001$; ·, indicates $0.5 \leq p < 0.1$, and -, indicates $p \geq 0.1$. *ITPR2*, Inositol 1,4,5-trisphosphate receptor type 2; OS, Overall survival.

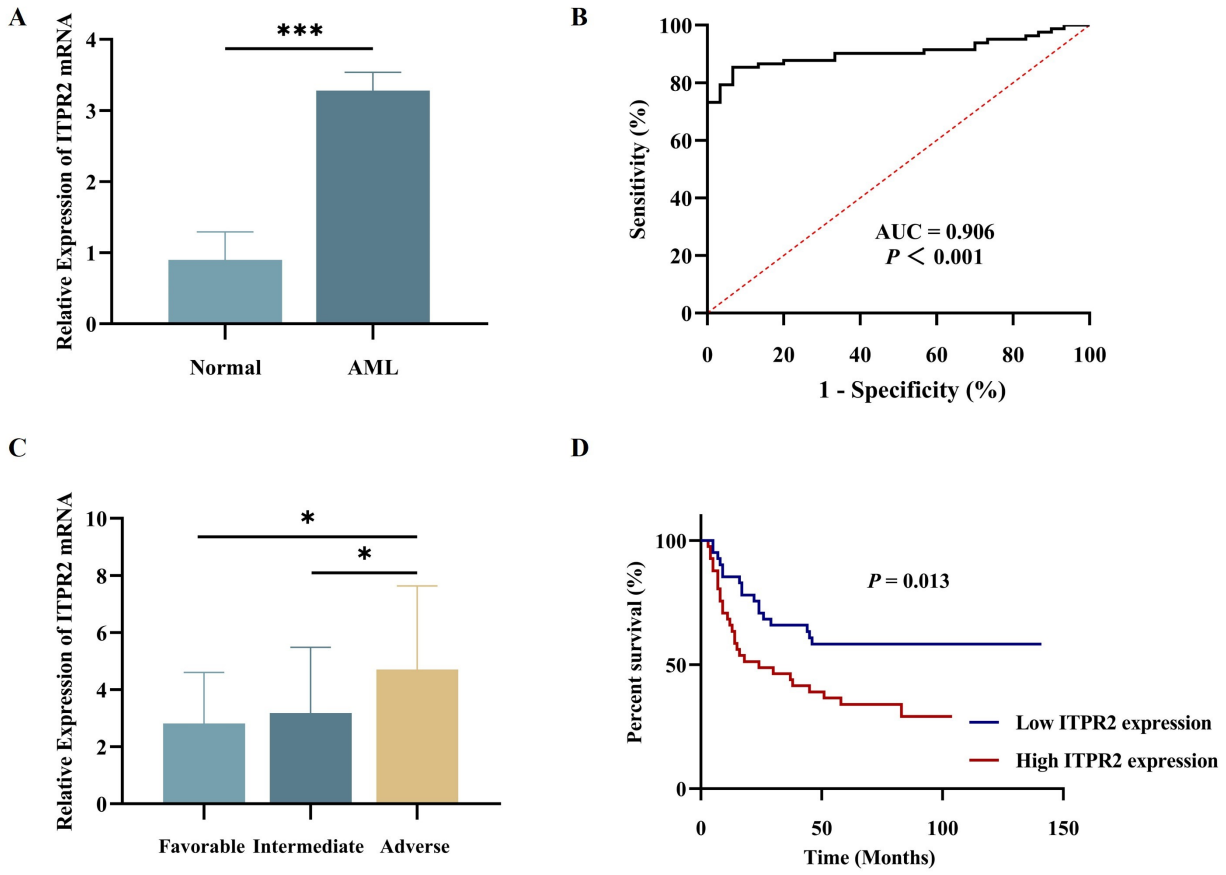

Fig. 2. *ITPR2* expression was increased in clinical samples vs. normal group and associated with clinical features. (A) The expression of *ITPR2* in AML patients (n = 82) and normal group (n = 30). (B) ROC analysis of *ITPR2* for diagnosing AML. (C) *ITPR2* expression associated with increasing risk stratification. (D) Kaplan-Meier analysis of AML patients showed significantly lower survival in the *ITPR2* high expression group compared with the low expression group. * $p < 0.05$, *** $p < 0.001$. AML, Acute myeloid leukemia; ROC, Receiver operating characteristic.

2.14 mtDNA Quantification

A Genomic DNA Mini Preparation Kit (Beyotime) was used to isolate total DNA from treated cells. Reactions for RT-qPCR were performed with Real Star Fast SYBR qPCR (Genstar, Shenzhen, China). Human β-actin was used as a reference gene to normal-

ize. The primer sequences were as follows: β-actin forward 5′-GTGGCCGAGGACTTTGATTG-3′ and reverse 5′-CCTGTAACAACGCATCTCATATT-3′, mt*ND1* forward 5′-CCCTAAAACCCGCCACATCT-3′ and reverse 5′-GAGCGATGGTGAGAGCTAAGGT-3′.

2.15 Drug Susceptibility Testing In Vitro

Cells were seeded in the medium containing varying concentrations of 2-Aminoethyl diphenylborinate (2-APB) or dimethyl sulfoxide (DMSO) control. After a specified incubation interval, 10 µL of CCK-8 reagent was added, and the plates were cultured for viability of the cells was determined according to this formula: cell viability rate = [(As–Ab)/(Ac–Ab)] $\times$ 100. The half maximal inhibitory concentration (IC50) was calculated using regression analysis with GraphPad Prism 8.0 software (GraphPad Software, Inc., San Diego, CA, USA) based on the cell viability data.

2.16 Statistical Analysis

Statistical analysis were performed on SPSS 25.0 (IBM Corp., Armonk, NY, USA) and GraphPad Prism 8.0 software. Each *in vitro* experiment was replicated a minimum of three times for every sample, repeat, group, and condition. The *t*-test was used to judge statistical variances in quantitative datasets. For nonparametric data, the Mann-Whitney U test was implemented. Correlations between two parameters were determined via the Pearson's analysis. The criteria of $p < 0.05$ was set to define statistical significance. Survival analyses were depicted via Kaplan-Meier plots, with log-rank tests for the significance in survival distributions.

3. Results

3.1 ITPR2 Is Upregulated in AML and Correlates With Poor Prognosis

Given the potential critical role of *ITPR2* in AML, we first investigated the expression profiles of *ITPR2* across malignancies. This research collected a harmonized pan-cancer dataset from the UCSC database, which revealed that *ITPR2* expression exhibits significant variations among multiple tumor types (Fig. 1A). To explore the clinical significance of *ITPR2* in AML prognosis, the gene expression and clinical data of 242 non-M3 AML patients from the GSE12417 dataset were downloaded. Kaplan–Meier analysis revealed that high *ITPR2* level was associated to significantly shorter OS (Fig. 1B)

To validate the results, BM samples and clinical data from 82 non-M3 AML patients and 30 healthy donors were collected. RT-qPCR analysis revealed significantly higher *ITPR2* expression in AML patients than in controls (Fig. 2A). Receiver operating characteristic (ROC) curve analysis revealed an area under the curve (AUC) of 0.906 (95% CI: 0.851–0.961, $p < 0.001$, Fig. 2B) for distinguishing AML patients from controls. To assess the clinical relevance of *ITPR2* in AML, the included cases were divided into favourable, intermediate, and adverse risk groups on the basis of diagnostic cytogenetic and molecular features. *ITPR2* expression increased with risk severity, with the lowest expression in the favourable group and the highest expression in the adverse risk group (Fig. 2C).

To further analysis the relationship between *ITPR2* expression and OS in AML patients, subjects were divided into low and high *ITPR2* expression groups with the median relative *ITPR2* expression as the cutoff. The Kaplan-Meier analysis indicated a significantly shorter OS in AML cases with high *ITPR2* level versus those with low *ITPR2* level (Fig. 2D). Table 1 compares the clinical and biological characteristics of the two groups. Notably, high *ITPR2* expression was significantly associated with a greater number of BM blasts ($p = 0.01$). The Cox regression analyses of the AML subgroups indicated that high *ITPR2* level was a significant independent factor for short OS ($p < 0.05$, Table 2).

3.2 Functional Enrichment and Immune Infiltration Analysis of ITPR2

To analysis the functional significance of *ITPR2* in AML, TCGA samples were divided into two different expression groups based on the median *ITPR2* level. Differential expression analysis was performed using the *limma* package. DEGs were screened with $|\log2FC| > 1$ and adjusted $p < 0.05$, followed by Gene Ontology (GO) and Kyoto Encyclopedia of Genes and Genomes (KEGG) analyses (Fig. 3A,B). GO analysis revealed that DEGs were significantly enriched in biological processes such as cellular immune responses and generation of superoxide anions; in cellular components such as cytoplasmic vesicle lumens; and molecular functions such as immune receptor activity, activation of nicotinamide adenine dinucleotide (Phosphate) reduced (NAD(P)H) oxidase activity, and Ca^{2+}-dependent protein binding. KEGG analysis revealed significant enrichment of DEGs in the B-cell receptor signalling pathway and haematopoietic cell lineage. In addition, DEGs from the *limma*-based differential analysis, screened with adjusted $p < 0.05$, were used for GSEA (Fig. 3C).

For the purpose of exploring *ITPR2*'s role in AML-related immune regulation, the ESTIMATE algorithm was utilized. Outcomes revealed an inverse association between *ITPR2* level and both the ESTIMATE and immune score (Fig. 3D–F). Using the ssGSEA algorithm, the correlation of *ITPR2* with the infiltration score was analysed (Fig. 3G). *ITPR2* level was positively related to the T helper and T-cell infiltration but negatively related to the Tregs, Th17 cells, macrophages, and NK CD56dim cells. Furthermore, the associations between *ITPR2* and immune checkpoint genes were evaluated through pearson correlation analysis. *ITPR2* was positively correlated with the expression of CD160, CD244, CD80, etc. (Fig. 3H–N).

Table 1. Comparisons of clinical features in AML patients.

Clinical characteristics	*ITPR2* level		*p* value
	Low (n = 41)	High (n = 41)	
Age (years), median (range)	37 (22–62)	32 (19–67)	0.388
Sex			0.656
Male	18	16	
Female	23	25	
Leukocyte, $\times 10^9$/L, median (range)	15.90 (0.49–182.50)	29.48 (0.09–242.10)	0.310
Hemoglobin, g/L, median (range)	77.80 (46.00–126.20)	72.60 (40.10–115.6)	0.926
Platelet, $\times 10^9$/L, median (range)	33.30 (8.00–168.60)	44.40 (7.00–237.10)	0.568
Bone marrow (BM) blasts, %, median (range)	51.50 (20.00–94.20)	69.00 (21.20–92.20)	0.010
FAB type, n (%)			0.679
M1	1 (2.44)	4 (9.76)	
M2	14 (34.15)	11 (26.83)	
M4	14 (34.15)	16 (39.02)	
M5	12 (29.26)	9 (21.95)	
M6	0 (0.00)	1 (2.44)	
Cytogenetic risk n (%)			0.061
Favorable	15 (36.58)	12 (29.27)	
Intermediate	23 (56.10)	20 (48.78)	
Adverse	3 (7.32)	9 (21.95)	
Mutation status, n (%)			
Nucleophosmin 1 (*NPM1*)			0.243
Mutation	9 (21.95)	5 (12.20)	
Wild type	32 (78.05)	36 (87.80)	
Fms-like Tyrosine Kinase 3 (*FLT3*)			0.801
Mutation	10 (24.39)	11 (26.83)	
Wild type	31 (75.61)	30 (73.17)	
DNA Methyltransferase 3 (*DNMT3*)			0.535
Mutation	7 (17.07)	5 (12.20)	
Wild type	34 (82.93)	36 (87.80)	
CCAAT/Enhancer Binding Protein Alpha (*CEBPA*)			0.193
Mutation	7 (17.07)	12 (29.27)	
Wild type	34 (82.93)	29 (70.73)	
Wilms Tumor 1 (*WT1*)			0.148
Mutation	15 (36.59)	9 (21.95)	
Wild type	26 (63.41)	32 (78.05)	
Hematopoietic stem cell transplantation (HSCT), n (%)			0.263
Yes	14 (34.15)	19 (46.34)	
No	27 (65.85)	22 (53.66)	
Complete remission, n (%)			0.355
Yes	29 (70.73)	25 (60.98)	
No	12 (29.27)	16 (39.02)	

FAB, French-American-British Classification System.

3.3 ITPR2 Knockdown Inhibits AML Cell Proliferation and Promotes Apoptosis

To clarify the role of *ITPR2* in AML, siRNAs were used to knockdown *ITPR2* in the THP-1 cell line. The knockdown efficiency was verified by RT-qPCR and WB (Fig. 4A,B). In functional validation experiments, CCK-8 assay data confirmed that *ITPR2* knockdown obviously blocked the proliferation of THP-1 cells (Fig. 4C). According to the result of flow cytometry, it was found that the loss of *ITPR2* caused an increase in the ratio of cells in the G0/G1 stage (Fig. 4D) and suggested a potential induction of apoptosis (Fig. 4E,F). WB analysis further verified that *ITPR2* knockdown not only reduced the expression of G1/S transition regulatory factors (cyclin D1, cyclin E1, and cyclin-dependent kinase 6 (CDK6)) but also downregulated the levels of Bcl-2 and Bcl-2-associated X protein (Bax) (Fig. 4G). While both Bcl-2 and Bax decreased, the resulting Bcl-2/Bax ratio <1 was shown to promote apoptosis in previous study [18].

To explore the treatment potential of targeting *ITPR2*, an *in vitro* drug sensitivity assay was performed. 2-APB is a specific inhibitor of *ITPRs* [19]. RT-qPCR and WB

Table 2. Analysis of single and multiple variables in AML patients.

Factor	Univariate		Multivariate	
	Hazard ratio (95% CI)	*p* value	Hazard ratio (95% CI)	*p* value
ITPR2 (high vs. low)	2.113 (1.155–3.866)	0.015	1.972 (1.073–3.622)	0.029
Age (<35 vs. ≥35)	1.494 (0.803–2.779)	0.205		
Sex (male vs. female)	0.994 (0.969–1.019)	0.614		
Leukocyte (<20 vs. ≥20)	0.835 (0.464–1.501)	0.547		
Hemoglobin, (<75 vs. ≥75)	0.758 (0.422–1.362)	0.355		
Platelet (<50 vs. ≥50)	1.346 (0.743–2.438)	0.327		
BM blasts (<65 vs. ≥65)	1.180 (0.655–2.126)	0.581		
NPM1 (mutated vs. wild)	0.700 (0.296–1.654)	0.416		
FLT3 (mutated vs. wild)	1.379 (0.711–2.675)	0.341		
DNMT3 (mutated vs. wild)	0.536 (0.192–1.497)	0.234		
CEBPA (mutated vs. wild)	1.131 (0.573–2.235)	0.722		
WT1 (mutated vs. wild)	0.479 (0.222–1.032)	0.060		
Cytogenetic risk (Favorable vs. Intermediate & adverse)	1.834 (0.945–3.559)	0.073		
Complete remission (yes vs. no)	6.149 (3.203–11.805)	<0.001	4.968 (2.464–10.018)	<0.001
HSCT (yes vs. no)	0.400 (0.206–0.775)	0.007	0.627 (0.306–1.285)	0.203

confirmed that 2-APB effectively inhibited the expression of *ITPR2* (Fig. 5A,B). The viability of THP-1 cells exposed to 2-APB was assessed with CCK-8 assays. The results revealed that prolonged drug exposure significantly decreased cell viability, with an IC50 value of 202 μM after 48 h (Fig. 5C). Therefore, in the subsequent experiments, this concentration and treatment time were selected for the subsequent tests. Additionally, the results of the cell proliferation assay indicated that compared with the control group, 2-APB led to more pronounced inhibition of cell growth (Fig. 5D). Flow cytometry analysis revealed that 2-APB increased the proportion of cells arrested in the G0/G1 phase (Fig. 5E) and suggested a potential induction of apoptosis (Fig. 5F,G). WB analysis further demonstrated that 2-APB treatment reduced the levels of cyclin D1, cyclin E1, Bcl-2, and Bax (Fig. 5H).

3.4 ITPR2 Knockdown Reduces Mitochondrial Ca^{2+} Levels and Promotes Mitochondrial Dysfunction

ITPR2 mediates Ca^{2+} transport. To investigate whether the aberrant upregulation of *ITPR2* in AML cells disrupts intracellular Ca^{2+} homeostasis, this research detected the cytosolic and mitochondrial Ca^{2+} levels via the Fluo-4 and Rhod-2 probes, respectively. Our results showed that compared with si-NC, si-*ITPR2* significantly reduced Ca^{2+} concentrations in both compartments (Fig. 6A,B). Mitochondrial Ca^{2+} imbalance will result in elevated oxidative stress and mitochondrial dysfunction. With the MMP-sensitive fluorescent dye JC-1, changes in the MMP were evaluated by analyzing the red/green fluorescence ratio. Knockdown of *ITPR2* significantly depolarized the MMP (Fig. 6C), a hallmark of mitochondrial dysfunction associated with early apoptosis. The intracellular ROS levels were determined using DCFH-DA. We found that *ITPR2* knockdown increased the level of intracellular ROS (Fig. 6D). To evaluate the effect of *ITPR2* on mtDNA-encoded respiratory chain gene expression, NADH dehydrogenase 1 (*ND1*) mRNA was quantified in THP-1 cells. Knockdown of *ITPR2* significantly downregulated *ND1* mRNA (Fig. 6E). These results are consistent with those in 2-APB-treated THP-1 cells (Fig. 6A–E).

4. Discussion

Recent studies have highlighted the oncogenic potential of *ITPR2* across various malignancies. The overexpression of *ITPR2* has been implicated in a poor prognosis for lung adenocarcinoma cases [20], renal cell carcinoma [21], and chronic lymphocytic leukaemia [22]. In lung cancer A549 cells, the overexpression of endoplasmic reticulum protein 44 (ERP44) reduces intracellular Ca^{2+} release via *ITPR2*, alters cell morphology, and significantly inhibits cell migration [23]. Zhang *et al.* [24] reported that Aflatoxin B1 (*AFB1*) induced pyroptosis in mouse livers by activating the caspase-12/caspase-3 pathway through *ITPR2* activation. The above findings indicate that *ITPR2* could serve as a novel target for the therapy of *AFB1*-induced liver injury. In breast cancer patients, *ITPR2* expression levels are specifically elevated in tumour tissues compared with adjacent nontumoral tissues. ITPR inhibition or siRNA-mediated silencing results in compromised bioenergetics and in increased ROS production and autophagy, which ultimately leads to cell death [4,23].

This study suggests that *ITPR2* may serve as a novel and critical therapeutic target for the therapy of AML. RT-qPCR results indicated that *ITPR2* expression was notably elevated in BM-MNCs from AML patients, with higher levels correlating with a worse prognosis and shorter OS. *ITPR2* supports proliferation in AML cells. This finding not only suggests that *ITPR2* may serve as a key driver molecule in AML progression but also supports its poten-

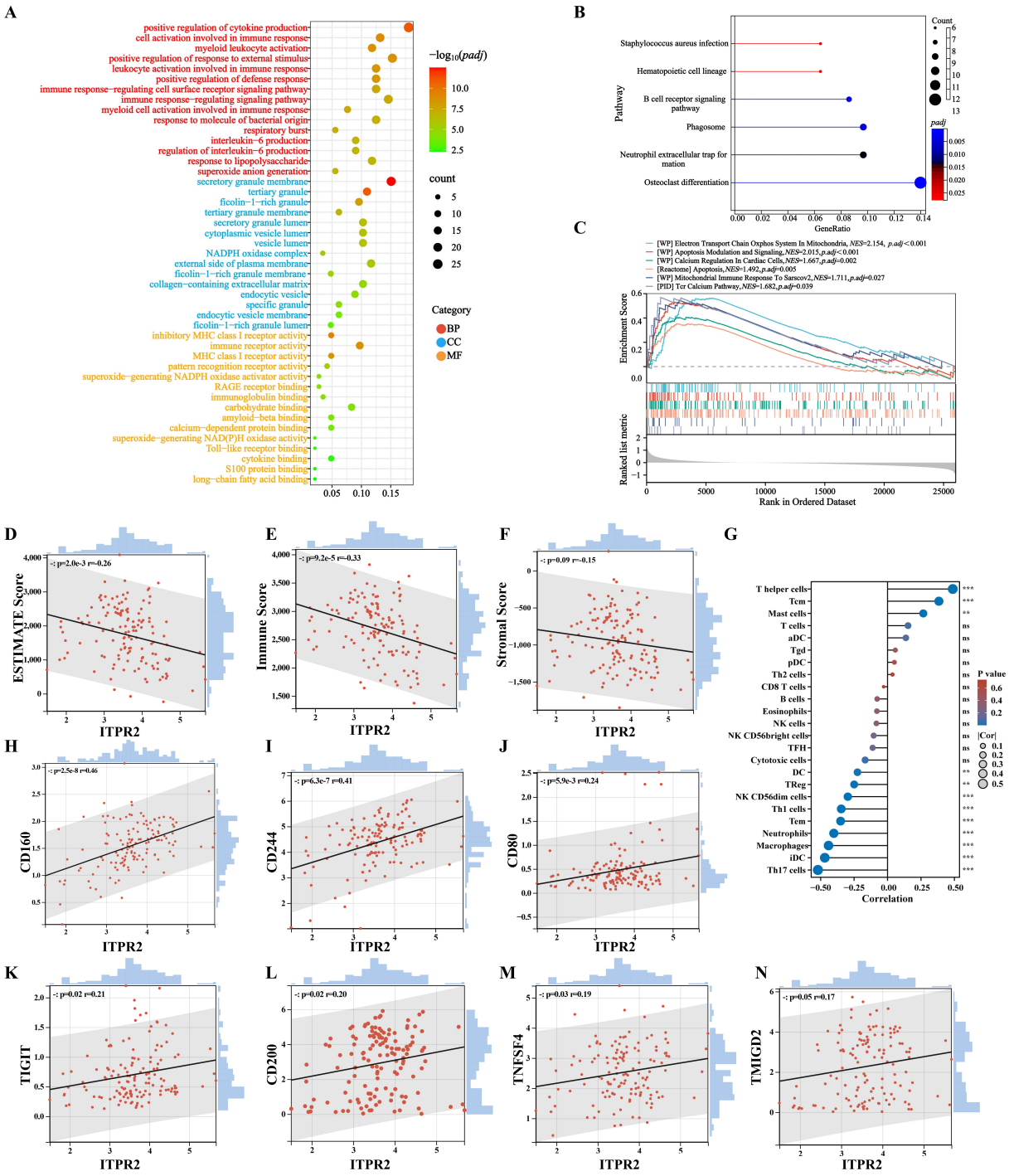

Fig. 3. Functional enrichment and immune infiltration analysis of *ITPR2* expression in TCGA-LAML patients. (A,B) GO and KEGG enrichment analysis of DEGs. (C) GSEA analysis of DEGs. (D–F) Correlation analysis of ESTIMATE score (D), immune score (E) and stromal score (F), respectively. (G) Correlation analysis of *ITPR2* with different immune cells. (H–N) Correlation between *ITPR2* and the immune checkpoint CD160 (H), CD244 (I), CD80 (J), *TIGIT* (K), CD200 (L), *TNFSF4* (M) and *TMIGD2* (N), respectively. ** $p < 0.01$, *** $p < 0.001$, ns: not significant ($p > 0.05$). TCGA-LAML, The Cancer Genome Atlas-Acute Myeloid Leukemia; GO, Gene Ontology; KEGG, Kyoto Encyclopedia of Genes and Genomes; DEGs, Differentially expressed genes; GSEA, Gene Set Enrichment Analysis; ESTIMATE, Estimation of Stromal and Immune cells in Malignant Tumor tissues using Expression data; *TIGIT*, T cell immunoreceptor with Ig and ITIM domains; *TNFSF4*, Tumor necrosis factor superfamily member 4; *TMIGD2*, Transmembrane and immunoglobulin domain containing 2.

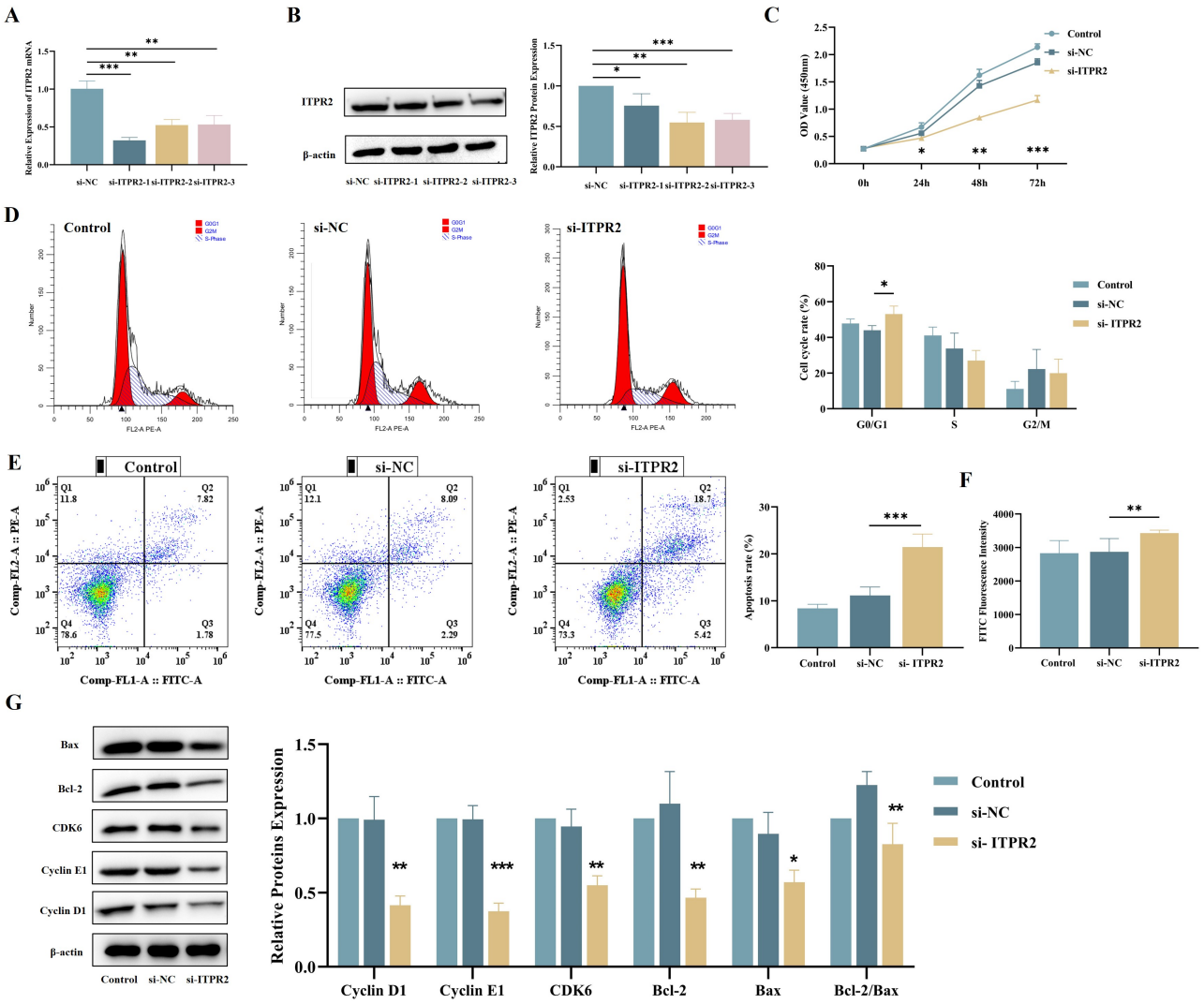

Fig. 4. siRNA-mediated *ITPR2* knockdown suppresses THP-1 cell proliferation and induces apoptosis. (A,B) RT-qPCR and WB analysis were employed to examine the efficiency of *ITPR2* knockdown in THP-1 cells (n = 3). (C) CCK-8 assay demonstrated that *ITPR2* knockdown inhibited THP-1 proliferation (n = 3). (D) Cell cycle distribution of *ITPR2*-knockdown THP-1 cells analyzed by flow cytometry (n = 3). (E,F) The apoptotic rate of *ITPR2* knockdown THP-1 cells was increased by using the Annexin V-FITC Apoptosis Detection Kit (E) and the One-step TUNEL Apoptosis Kit (n = 3) (F) for cell staining separately through flow cytometry. (G) WB analysisdemonstrated the expression levels of cell cycle and apoptosis-related proteins in *ITPR2* knockdown cells. Grayscale values were quantified using ImageJ. The quantitative results of the levels of cycle and apoptosis-related proteins were adjusted using the level of β-actin protein. The image represents one of the 3 independent parallel experiments. Data were normalized to the Control group, so error bars are not included for the Control group. si-, small interfering; Control, THP-1 cells without any treatment; NC, negative control; Compared with si-NC, * $p < 0.05$, ** $p < 0.01$, *** $p < 0.001$. RT-qPCR, Quantitative real-time PCR; WB, Western blot; THP-1, Tohoku Hospital Pediatrics-1; CCK-8, Cell counting kit-8; V-FITC, V-Fluorescein Isothiocyanate; TUNEL, Terminal Deoxynucleotidyl Transferase dUTP Nick-End Labeling; CDK6, Cyclin-dependent kinase 6; Bcl-2, B-cell lymphoma-2; Bax, Bcl-2-associated X protein.

tial as a prognostic biomarker, thereby further expanding the clinical implications of *ITPR2* in hematological malignancies.

Immune dysregulation is one of the key mechanisms underlying the progression and therapeutic resistance of AML. To investigate the function of *ITPR2* in AML, we first focused on its association with the AML immune microenvironment to uncover the potential mechanisms by which it regulates disease progression. Results from immune scoring and ESTIMATE analysis indicated that *ITPR2* level was obvious negatively related to these scores, suggesting that *ITPR2* may be involved in the formation of an immunosuppressive tumor microenvironment (TME) by regulating immune cell infiltration. Further ss-

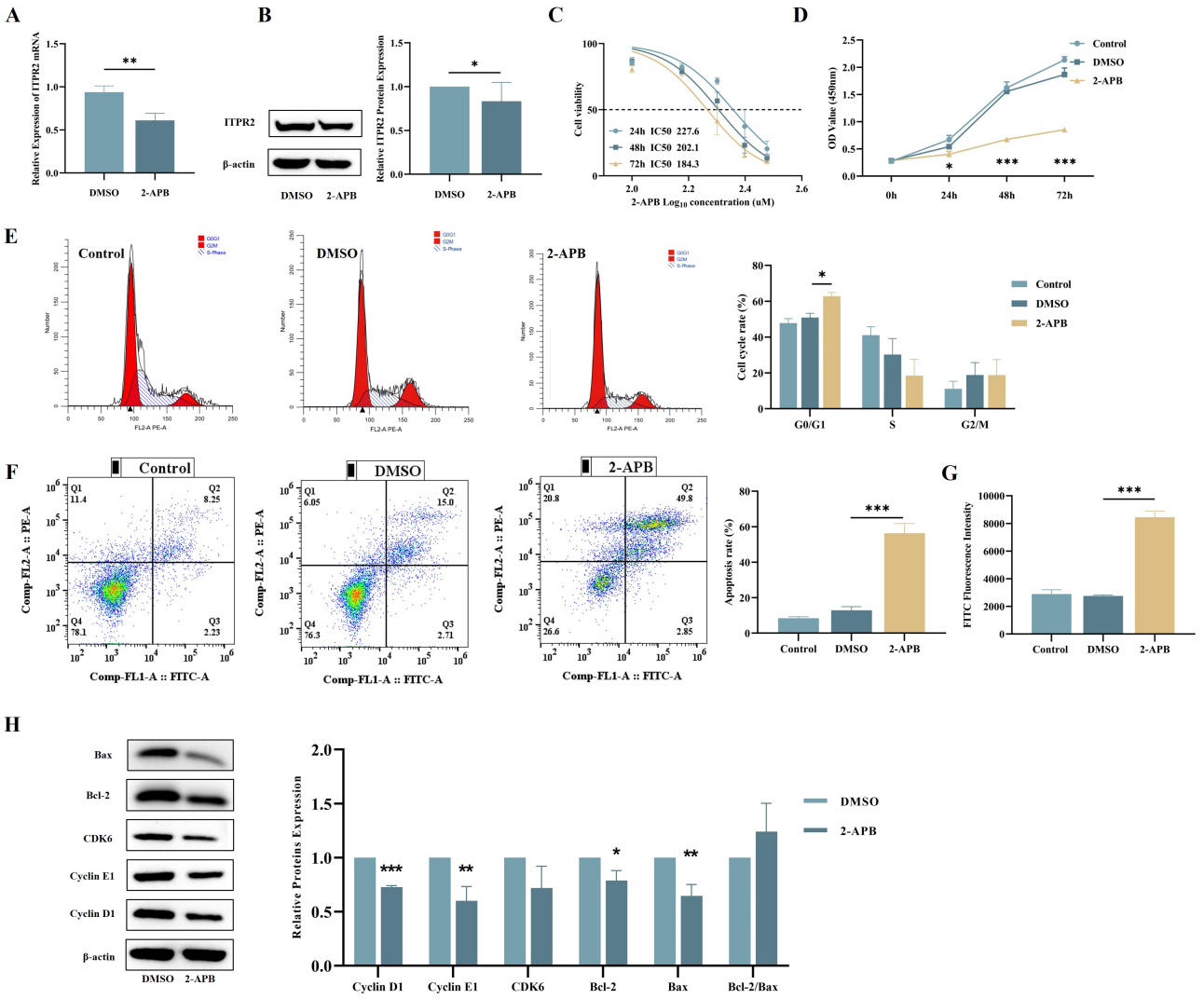

Fig. 5. Exposure of THP-1 cells to 200 µM 2-APB for 48 h resulted in impaired proliferation and enhanced apoptosis. (A,B) RT-qPCR and WB analysis of THP-1 cells treated with 2-APB revealed decreased *ITPR2* expression (n = 3). (C) Effect of different concentrations of 2-APB on the cell viability of THP-1 cell line (n = 6). (D) CCK-8 assay demonstrated 2-APB treatment effectively suppressed THP-1 growth (n = 3). (E) Cell cycle distribution of 2-APB-treated THP-1 cells analyzed by flow cytometry (n = 3). (F,G) The apoptotic rate of 2-APB-treated THP-1 cells was increased by using the Annexin V-FITC Apoptosis Detection Kit (F) and the One-step TUNEL Apoptosis Kit (G) for cell staining separately through flow cytometry (n = 3). (H) WB examined cell cycle and apoptosisrelated protein expression in 2-APB-treated THP-1 cells. Grayscale values were quantified using ImageJ. The quantitative results of the levels of cycle and apoptosis-related proteins were adjusted using the level of β-actin protein. The image represents one of the 3 independent parallel experiments. Data were normalized to the DMSO group, so error bars are not included for the DMSO group. Compared with DMSO, * $p < 0.05$, ** $p < 0.01$, *** $p < 0.001$. 2-APB, 2-Aminoethyl diphenylborinate; DMSO, Dimethyl sulfoxide; IC50, Half maximal inhibitory concentration.

GSEA revealed that *ITPR2* was positively correlated with T helper cells and central memory T cells, while negatively correlated with innate immune cells (e.g., dendritic cells (DCs)/immature DCs (iDCs), etc.), effector memory T cells, Th1/Th17 cells, regulatory T cells. Notably, as immune memory cells, the enrichment of Tcm may increase the risk of AML recurrence, whereas the reduction of Th1/Th17 cells impairs antitumor immune responses. This bidirectional regulatory pattern is relatively rare among other tumor-related molecules, indicating that *ITPR2* exerts a unique role in shaping the immune landscape of the AML TME.

Immune checkpoint molecules such as T cell immunoreceptor with Ig and ITIM domains (*TIGIT*), CD160, and CD244 are predominantly expressed on the T cells and NK cells. These molecules transmit inhibitory signals

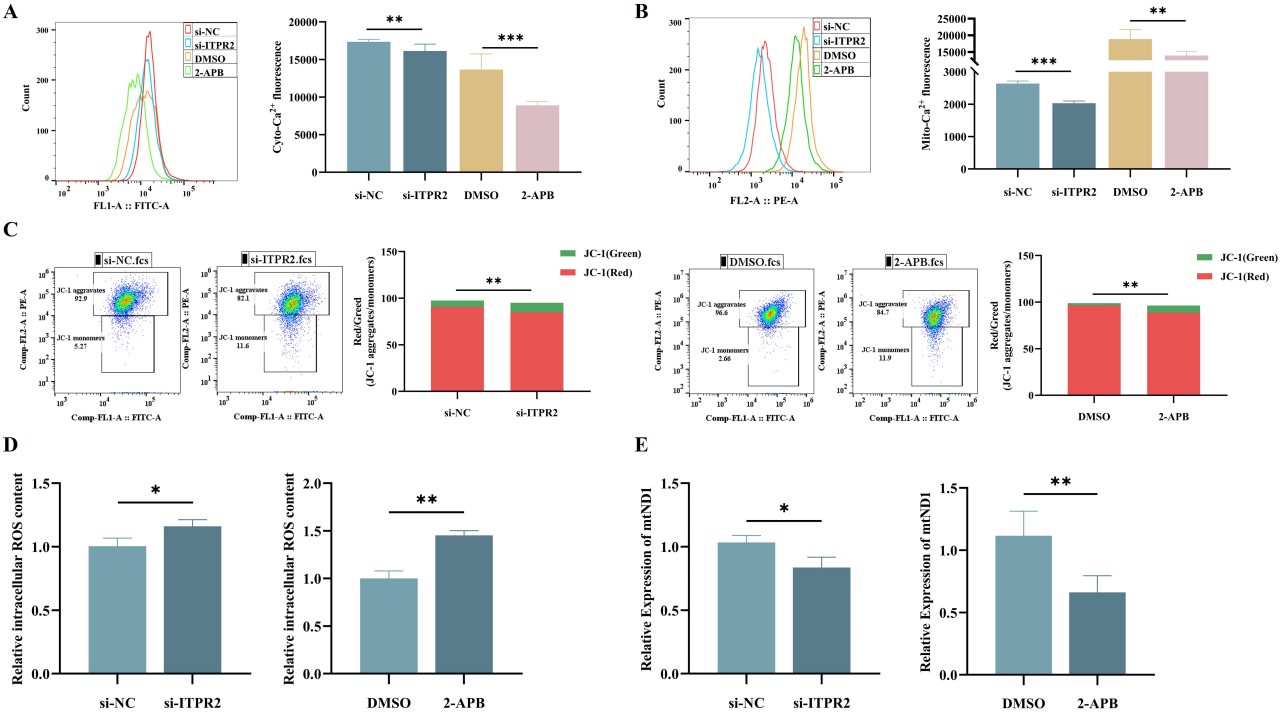

Fig. 6. *ITPR2* Knockdown and 2-APB treatment reduce intracellular Ca^{2+} and induce mitochondrial dysfunction in THP-1 Cells. (A,B) Flow cytometric analysis revealed reduced intracellular Ca^{2+} (A) and mitochondrial Ca^{2+} (B) levels in THP-1 cells after *ITPR2* knockdown or 2-APB treatment. (C) Flow cytometry showed reduced MMP in THP-1 cells following *ITPR2* knockdown or 2-APB treatment. (D) Flow cytometry showed increased ROS levels in THP-1 cells following *ITPR2* knockdown or 2-APB treatment. (E) RT-qPCR showed reduced mt*ND1* expression in THP-1 cells with *ITPR2* knockdown or 2-APB treatment. The image represents one of the 3 independent parallel experiments. si-, small interfering; NC, negative control. Compared with si-NC or DMSO * $p < 0.05$, ** $p < 0.01$, *** $p < 0.001$. Ca^{2+}, Calcium; MMP, Mitochondrial membrane potential.

through binding to their ligands, which induces immune cell exhaustion, impairing their ability to recognize and kill tumour cells, and thus represents a key mechanism underlying tumour immune evasion. A preclinical research indicated that tumour-infiltrating *TIGIT*+ NK cells were exhausted in transplant mouse tumour models and that blockade of *TIGIT* can unleash the antitumour function of NK cells and promote the CD8+ T-cell antitumour response. The blockade of *TIGIT* alone or combined with anti-programmed cell death protein 1 (anti-PD-1) or anti-programmed death-ligand 1 (anti-PD-L1) blockade is being tested in many clinical trials [25,26], highlighting its value of treatment target. In AML, high level of CD244 may associate with the construction of an immunosuppressive TME by inducing T-cell depletion, which impairs the antileukaemia function of these cells [27]. A similar mechanism has also been observed in chronic lymphocytic leukemia (CLL). It has been reported that higher level of CD244, PD-1, CD160 on the T cells of untreated CLL cases, is often accompanied by abnormal of cytotoxicity [28]. Here, we found that the abovementioned immune checkpoint molecules were significantly positively correlated with *ITPR2*, suggesting that *ITPR2* may directly inhibit the immune activity of T and NK cells and indirectly promote the immune escape of tumour cells through the upregulation of the expression of these molecules. On the basis of this correlation, *ITPR2* can be seemed as a predictor for the efficacy of relevant immunotherapies.

Beyond its immunomodulatory function, the regulation of malignant phenotypes in AML cells by *ITPR2* also relies on its core regulation of mitochondrial function. Previous studies have demonstrated that upregulated *ITPR2* promotes massive Ca^{2+} influx into mitochondria, leading to abnormal elevation of Ca^{2+} concentration in the mitochondrial matrix. This alteration activates Ca^{2+}-dependent enzymes in mitochondria, thereby impairing mitochondrial respiratory chain function. Inhibition of ITPR and Ca^{2+} transfer to mitochondria causes cell cycle arrest and cell death in T-cell acute lymphoblastic leukaemia cells [29]. In AML cell lines, elevated mitochondrial Ca^{2+} levels are observed in cells that can evade treatment with cytarabine and venetoclax [30]. Zhong *et al.* [31] reported that abnormally increased expression of oxysterol-binding protein-related protein 4L (ORP4L) can activate *ITPRs*, leading to ER Ca^{2+} release to increase mitochondrial respiration and promote the survival of leukaemia stem cells

[32]. Our experimental data demonstrated that targeted knockdown of *ITPR2* significantly reduced mitochondrial Ca^{2+} uptake and induced depolarization of MMP ($\Delta\psi$m) in AML cells—a typical hallmark of mitochondrial dysfunction. Impaired mitochondrial structure and function further inhibited the activity of electron transport chain complexes, leading to increased intracellular ROS production, which was highly consistent with the "mitochondrial electron transport chain and oxidative phosphorylation" pathway identified by GSEA enrichment analysis. In addition, the expression level of *ND1*, a gene associated with mitochondrial copy number, was significantly downregulated following *ITPR2* knockdown. Given that mtDNA stability is directly linked to mitochondrial function, the reduced *ND1* expression further corroborates the disruptive effect of *ITPR2* knockdown on mitochondrial structure and function. Collectively, these results indicate that *ITPR2* promotes AML cell proliferation by mediating Ca^{2+} homeostasis and regulating mitochondrial functional homeostasis in AML cells, defining the core molecular mechanism underlying its oncogenic role.

Modulation of ion channels (both inhibition and activation) in cells and their organelles, as well as the modulation of cell redox states, has been used to treat various diseases. 2-APB, one of the most extensively studied boron-containing compounds, is capable of modulating the activities of a variety of ion channels and is used as an inhibitor of *ITPRs* [33]. 2-APB has been demonstrated to inhibit Ca^{2+} uptake by isolated liver mitochondria in a dose-dependent manner and to reduce cellular Ca^{2+} accumulation in hepatocellular carcinoma G2 cells [34]. In the present study, 2-APB, by inhibiting *ITPR2* function, also induces reduced mitochondrial Ca^{2+} uptake, mitochondrial dysfunction, and ultimately AML cell apoptosis in AML cells. Given that *ITPR2* is highly expressed in AML patients and associated with poor prognosis, these findings collectively confirm the potential feasibility of *ITPR2* as a therapeutic target for AML, providing critical experimental evidence for the development of *ITPR2*-targeted therapeutic strategies. However, its clinical translational value requires further validation through in-depth follow-up studies.

Severals limitations of this study should be acknowledged. Firstly, confining the study to the THP-1 cell line, which lacks cell type diversity, and assessing only a restricted range of apoptotic markers (e.g., excluding the evaluation of cleaved caspase-3 and other essential apoptotic proteins) may constrain the generalizability of our findings. Therefore, forthcoming research will expand the variety of cell types and apoptotic markers for assessment, explore further the signaling pathways accountable for the observed effects. Secondly, we could not validate the *in vitro* results in AML primary cells. In the future, we will isolate primary cells from AML patients following standardized clinical processing and validation protocols, and corroborate the outcomes from THP-1 cell line experiments in the patient samples encompassed in the study. Thirdly, due to constraints in experimental duration and resources, *in vivo* validation remains incomplete. Complex *in vivo* microenvironment, such as immune regulation and intertissue crosstalk, may alter *ITPR2*-mediated molecular mechanisms and drug responses, necessitating further verification of *in vitro* findings using *in vivo* models. Additionally, the pharmacokinetic and pharmacodynamic properties of 2-APB *in vivo*—such as its bioavailability, tissue distribution, metabolism, and off-target effects—may differ substantially from its performance in cell culture systems, which could impact its actual therapeutic potential and safety profile. Therefore, future studies should prioritize validating these observations using relevant preclinical models, including AML xenograft mice, patient-derived xenograft models, or conditional *ITPR2* knockout models, to confirm the physiological significance of *ITPR2* in AML progression and rigorously evaluate the *in vivo* efficacy and safety of *ITPR2*-targeted therapies.

5. Conclusion

This study systematically clarifies the core role and clinical value of *ITPR2* in AML, offering an innovative perspective. Mechanistically, we first demonstrate that *ITPR2* drives AML progression via two pathways: (1) maintaining mitochondrial integrity through regulating Ca^{2+} transport via the "Ca^{2+} signaling-mitochondrial homeostasis" axis to promote proliferation and inhibit apoptosis; (2) establishing an immunosuppressive microenvironment by modulating immune cell infiltration and checkpoint molecules (e.g., *TIGIT*) to facilitate immune escape. The small-molecule inhibitor 2-APB targets *ITPR2* to induce AML cell mitochondrial dysfunction and apoptosis, supporting *ITPR2* as a potential therapeutic target. While lacking *in vivo* validation, this work provides a new basis for AML prognostic stratification and *ITPR2*-targeted strategies, with subsequent preclinical studies to solidify its clinical translation.

Availability of Data and Materials

The data generated in the present study may be requested from the corresponding author.

Author Contributions

XH and NL conducted most of the experiments and wrote the manuscripts. SZ collected and confirmed the authenticity of all raw data. XL analyzed the data. YH drew the pictures. JL completed the tables. ZL designed the study and critically revised the manuscript. All authors have read and approved the final version of the manuscript. All authors contributed to editorial changes in the manuscript. All authors have participated sufficiently in the work and agreed to be accountable for all aspects of the work.

Ethics Approval and Consent to Participate

This research has been reviewed and approved by the Ethical Review Commission of the First Affiliated Hospital of Guangxi Medical University, Nanning, China (Approval code: 2025-E0668). The Ethical Review Commission of the First Affiliated Hospital of Guangxi Medical University approved this study protocol and waived the obligation for informed consent because of the retrospective nature of the study. This study was conducted in accordance with the ethical standards of the Declaration of Helsinki.

Acknowledgment

The authors sincerely thank the patients whose valuable data were vital to this research.

Funding

This work was supported by the National Natural Science Foundation of China (No. 82160039 and No. 82560035), the Natural Science Foundation of Guangxi Province (No. 2025GXNSFAA069052), the Open Research Project from Key Laboratory of Clinical Laboratory Medicine of Guangxi Department of Education (No. GXGXLCJYZDX2025007), and the Middle-aged and Young Teachers' Basic Ability Promotion Project of Guangxi (No. 2024KY0112).

Conflict of Interest

The authors declare no conflict of interest.

References

[1] Bhansali RS, Pratz KW, Lai C. Recent advances in targeted therapies in acute myeloid leukemia. Journal of Hematology & Oncology. 2023; 16: 29. https://doi.org/10.1186/s13045-023-01424-6.

[2] Bohl SR, Bullinger L, Rücker FG. New Targeted Agents in Acute Myeloid Leukemia: New Hope on the Rise. International Journal of Molecular Sciences. 2019; 20: 1983. https://doi.org/10.3390/ijms20081983.

[3] Ando H, Kawaai K, Bonneau B, Mikoshiba K. Remodeling of Ca^{2+} signaling in cancer: Regulation of inositol 1,4,5-trisphosphate receptors through oncogenes and tumor suppressors. Advances in Biological Regulation. 2018; 68: 64–76. https://doi.org/10.1016/j.jbior.2017.12.001.

[4] Parys JB, Bultynck G, Vervliet T. IP_3 Receptor Biology and Endoplasmic Reticulum Calcium Dynamics in Cancer. Progress in Molecular and Subcellular Biology. 2021; 59: 215–237. https://doi.org/10.1007/978-3-030-67696-4_11.

[5] Han B, Zhen F, Zheng XS, Hu J, Chen XS. Systematic analysis of the expression and prognostic value of ITPR1 and correlation with tumor infiltrating immune cells in breast cancer. BMC Cancer. 2022; 22: 297. https://doi.org/10.1186/s12885-022-09410-w.

[6] Ueasilamongkol P, Khamphaya T, Guerra MT, Rodrigues MA, Gomes DA, Kong Y, *et al*. Type 3 Inositol 1,4,5-Trisphosphate Receptor Is Increased and Enhances Malignant Properties in Cholangiocarcinoma. Hepatology (Baltimore, Md.). 2020; 71: 583–599. https://doi.org/10.1002/hep.30839.

[7] Wu X, Scelo G, Purdue MP, Rothman N, Johansson M, Ye Y, *et al*. A genome-wide association study identifies a novel susceptibility locus for renal cell carcinoma on 12p11.23. Human Molecular Genetics. 2012; 21: 456–462. https://doi.org/10.1093/hmg/ddr479.

[8] Wu W, Shi Z, Tang Z, Li H, Huang X, Liang X, *et al*. Characterization of bone marrow heterogeneity in NK-AML (M4/M5) based on single-cell RNA sequencing. Experimental Hematology & Oncology. 2023; 12: 25. https://doi.org/10.1186/s40164-023-00391-5.

[9] Shi JL, Fu L, Wang WD. High expression of inositol 1,4,5-trisphosphate receptor, type 2 (ITPR2) as a novel biomarker for worse prognosis in cytogenetically normal acute myeloid leukemia. Oncotarget. 2015; 6: 5299–5309. https://doi.org/10.18632/oncotarget.3024.

[10] MacCannell D, Berger Z, Kirschner J, Mercuri E, Farrar MA, Iannaccone ST, *et al*. Restoration of Nusinersen Levels Following Treatment Interruption in People With Spinal Muscular Atrophy: Simulations Based on a Population Pharmacokinetic Model. CNS Drugs. 2022; 36: 181–190. https://doi.org/10.1007/s40263-022-00899-0.

[11] Yang S, Hui TL, Wang HQ, Zhang X, Mi YZ, Cheng M, *et al*. High expression of autophagy-related gene *EIF4EBP1* could promote tamoxifen resistance and predict poor prognosis in breast cancer. World Journal of Clinical Cases. 2023; 11: 4788–4799. https://doi.org/10.12998/wjcc.v11.i20.4788.

[12] Lima AS, Bezerra MF, Moreira-Aguiar A, Weinhäuser I, Santos BL, Falcão RM, *et al*. Prognostic implications of the ID1 expression in acute myeloid leukemia patients treated in a resource-constrained setting. Hematology, Transfusion and Cell Therapy. 2024; 46: 250–255. https://doi.org/10.1016/j.htct.2023.04.005.

[13] Bindea G, Mlecnik B, Tosolini M, Kirilovsky A, Waldner M, Obenauf AC, *et al*. Spatiotemporal dynamics of intratumoral immune cells reveal the immune landscape in human cancer. Immunity. 2013; 39: 782–795. https://doi.org/10.1016/j.immuni.2013.10.003.

[14] Danilova L, Ho WJ, Zhu Q, Vithayathil T, De Jesus-Acosta A, Azad NS, *et al*. Programmed Cell Death Ligand-1 (PD-L1) and CD8 Expression Profiling Identify an Immunologic Subtype of Pancreatic Ductal Adenocarcinomas with Favorable Survival. Cancer Immunology Research. 2019; 7: 886–895. https://doi.org/10.1158/2326-6066.CIR-18-0822.

[15] Zhao Q, Wang Q, Wang T, Xu J, Li T, Liu Q, *et al*. Pattern Recognition Receptors (PRRs) in Macrophages Possess Prognosis and Immunotherapy Potential for Melanoma. Frontiers in Immunology. 2021; 12: 765615. https://doi.org/10.3389/fimmu.2021.765615.

[16] Tsang SM, Kim H, Oliemuller E, Newman R, Boateng NA, Guppy N, *et al*. Sox11 regulates mammary tumour-initiating and metastatic capacity in Brca1-deficient mouse mammary tumour cells. Disease Models & Mechanisms. 2021; 14: dmm046037. https://doi.org/10.1242/dmm.046037.

[17] Qian X, Wang Y, Liu Z, Fang F, Ma Y, Zhou L, *et al*. Establishment of XRD fourier fingerprint identification method of realgar decoction pieces and its anti-tumor activity in tumor-in-situ transplanted mice. Journal of Ethnopharmacology. 2024; 331: 118303. https://doi.org/10.1016/j.jep.2024.118303.

[18] Moradi A, Abdihaji M, Kouchaksaraie SB, Alkinani TA, Mahmoudi A, Davoudi A, *et al*. Synthesize of Bi_2O_3/Gln-TSC nanoparticles and evaluation of their toxicity on prostate cancer cells and expression of CASP8, BAX, and Bcl-2 genes. Scientific Reports. 2022; 12: 21245. https://doi.org/10.1038/s41598-022-25360-6.

[19] Gu W, Ma X, Yang C, Jiang D, Fan H, Wang L, *et al*. Insight into Ca^{2+}- inositol 1,4,5-trisphosphate receptor 2 (IP_3R2)-mediated unfolded protein response and apoptosis in scallop Patinopecten yessoensis under high temperature stress. Comparative Biochemistry and Physiology. Part B, Biochemistry &

Molecular Biology. 2025; 278: 111092. https://doi.org/10.1016/j.cbpb.2025.111092.

[20] Huang X, Jin M, Chen YX, Wang J, Zhai K, Chang Y, *et al*. ERP44 inhibits human lung cancer cell migration mainly via IP3R2. Aging. 2016; 8: 1276–1286. https://doi.org/10.18632/aging.100984.

[21] Zhang N, Wu Y, Gong J, Li K, Lin X, Chen H, *et al*. Germline genetic variations in PDZD2 and ITPR2 genes are associated with clear cell renal cell carcinoma in Chinese population. Oncotarget. 2017; 8: 24196–24201. https://doi.org/10.18632/oncotarget.6917.

[22] Akl H, Monaco G, La Rovere R, Welkenhuyzen K, Kiviluoto S, Vervliet T, *et al*. IP3R2 levels dictate the apoptotic sensitivity of diffuse large B-cell lymphoma cells to an IP3R-derived peptide targeting the BH4 domain of Bcl-2. Cell Death & Disease. 2013; 4: e632. https://doi.org/10.1038/cddis.2013.140.

[23] Singh A, Chagtoo M, Tiwari S, George N, Chakravarti B, Khan S, *et al*. Inhibition of Inositol 1, 4, 5-Trisphosphate Receptor Induce Breast Cancer Cell Death Through Deregulated Autophagy and Cellular Bioenergetics. Journal of Cellular Biochemistry. 2017; 118: 2333–2346. https://doi.org/10.1002/jcb.25891.

[24] Zhang Y, Wang Y, Yang Y, Zhao D, Liu R, Li S, *et al*. Proteomic analysis of ITPR2 as a new therapeutic target for curcumin protection against AFB1-induced pyroptosis. Ecotoxicology and Environmental Safety. 2023; 260: 115073. https://doi.org/10.1016/j.ecoenv.2023.115073.

[25] Liu G, Zhang Q, Yang J, Li X, Xian L, Li W, *et al*. Increased TIGIT expressing NK cells with dysfunctional phenotype in AML patients correlated with poor prognosis. Cancer Immunology, Immunotherapy: CII. 2022; 71: 277–287. https://doi.org/10.1007/s00262-021-02978-5.

[26] Zhang Q, Bi J, Zheng X, Chen Y, Wang H, Wu W, *et al*. Blockade of the checkpoint receptor TIGIT prevents NK cell exhaustion and elicits potent anti-tumor immunity. Nature Immunology. 2018; 19: 723–732. https://doi.org/10.1038/s41590-018-0132-0.

[27] Huang S, Liang C, Zhao Y, Deng T, Tan J, Zha X, *et al*. Increased TOX expression concurrent with PD-1, Tim-3, and CD244 expression in T cells from patients with acute myeloid leukemia. Cytometry. Part B, Clinical Cytometry. 2022; 102: 143–152. https://doi.org/10.1002/cyto.b.22049.

[28] Schnorfeil FM, Lichtenegger FS, Emmerig K, Schlueter M, Neitz JS, Draenert R, *et al*. T cells are functionally not impaired in AML: increased PD-1 expression is only seen at time of relapse and correlates with a shift towards the memory T cell compartment. Journal of Hematology & Oncology. 2015; 8: 93. https://doi.org/10.1186/s13045-015-0189-2.

[29] Bustos G, Ahumada-Castro U, Silva-Pavez E, Puebla A, Lovy A, Cesar Cardenas J. The ER-mitochondria Ca^{2+} signaling in cancer progression: Fueling the monster. International Review of Cell and Molecular Biology. 2021; 363: 49–121. https://doi.org/10.1016/bs.ircmb.2021.03.006.

[30] Sheth AI, Althoff MJ, Tolison H, Engel K, Amaya ML, Krug AE, *et al*. Targeting Acute Myeloid Leukemia Stem Cells through Perturbation of Mitochondrial Calcium. Cancer Discovery. 2024; 14: 1922–1939. https://doi.org/10.1158/2159-8290.CD-23-1145.

[31] Zhong W, Xu M, Li C, Zhu B, Cao X, Li D, *et al*. ORP4L Extracts and Presents PIP_2 from Plasma Membrane for PLCβ3 Catalysis: Targeting It Eradicates Leukemia Stem Cells. Cell Reports. 2019; 26: 2166–2177.e9. https://doi.org/10.1016/j.celrep.2019.01.082.

[32] Monaco G, Percio S, Ting SB. Budgeting at the Ca^{2+} store: a $PIP_{(2)}$eline to starve LSCs? Cell Calcium. 2021; 93: 102309. https://doi.org/10.1016/j.ceca.2020.102309.

[33] Dubinin MV, Chulkov AV, Igoshkina AD, Cherepanova AA, Mikina NV. Effect of 2-aminoethoxydiphenyl borate on the functions of mouse skeletal muscle mitochondria. Biochemical and Biophysical Research Communications. 2024; 712–713: 149944. https://doi.org/10.1016/j.bbrc.2024.149944.

[34] Nicoud IB, Knox CD, Jones CM, Anderson CD, Pierce JM, Belous AE, *et al*. 2-APB protects against liver ischemia-reperfusion injury by reducing cellular and mitochondrial calcium uptake. American Journal of Physiology. Gastrointestinal and Liver Physiology. 2007; 293: G623–G630. https://doi.org/10.1152/ajpgi.00521.2006.